CONF-851102--8

ATFSR: A SMALL TORSATRON REACTOR*

W. A. Houlberg, J. T. Lacatski, and N. A. Uckan
Oak Ridge National Laboratory
P.O. Box Y
Oak Ridge, Tennessee 37831

CONF-851102--8

DE86 003010

Abstract. A small (average minor radius $\bar{a} \simeq 1$ m), moderate-aspect-ratio torsatron reactor based on the Advanced Toroidal Facility (ATF) is proposed as a starting point for improved stellarator reactor designs. The major limitation of the compact size is the lack of space under the helical coils for the blanket and shield. Neoclassical confinement models for helically trapped particles show that a large electric potential (radial electric field) is necessary to achieve ignition in a device of this size, although high-Q operation is still attainable with more modest potentials.

I. Introduction

Stellarator/torsatron reactors have the advantage of operating with zero net plasma current and steady-state magnetic fields, thus greatly reducing cyclic stresses and fatigue. Other advantages are disruption-free operation, natural divertor capabilities, startup on existing magnetic surfaces, and possible modular construction. Torsatrons have the additional advantage of improved access, since they require only ℓ helical windings to produce a poloidal harmonic of ℓ as opposed to 2ℓ windings in a stellarator. The reactor-relevant issues addressed here are the same issues faced by other magnetic confinement concepts: plasma beta (efficient use of the magnetic fields); engineering (size, access, shielding, etc.); and energy confinement (ignition or high-Q operation).

The ATF torsatron [1] should give direct access to the second stability regime (high beta) because of its moderate aspect ratio, its shear, and the stabilizing influence of the magnetic axis shift [2]. The lower aspect ratio of the ATF in combination with higher beta capabilities should then lead to more compact reactors than those considered in earlier power reactor studies [3]. Parameters for some of these are shown in Table I and compared with the results of this study, the ATF Stellarator Reactor (ATFSR) [4]. We start with ATF, scale it up to an average plasma minor radius of $\bar{a} = 1$ m, then examine the confinement and engineering issues that have an impact on feasibility. The ATF magnetic field and MHD properties are summarized and scaled up for the ATFSR in Section II. Recently developed theoretical models [5] and experiments on Wendelstein VII-A [6] have shown the importance of a radial electric field for confinement; the impact of these results on ATFSR is discussed in Section III. Section IV is a summary of results.

II. Magnetic Properties

The ATF torsatron is an $\ell = 2$ (2 helical coils), $m = 12$ (12 toroidal field periods) design with additional inner, middle, and outer vertical field (VF) coils, as shown in Fig. 1. For confinement studies, the magnetic field strength can be approximated as

$$B \simeq B_0[1 - \epsilon_t\cos\theta - \epsilon_h\cos(\ell\theta - m\phi)] ,$$

where the toroidal modulation is given by the local inverse aspect ratio, $\epsilon_t \simeq \rho/R_0$, and the helical modulation is

$$\epsilon_h \simeq \epsilon_{h0} + \epsilon_{ha}(\rho/\bar{a})^2$$

with $0 \leq \rho \leq \bar{a}$. Table II summarizes the dimensionless machine parameters that ATF and ATFSR have in common and also the scaled sizes, fields, and currents. The size has been scaled by a factor of 10/3 and the magnetic field by a factor of 5/2; coil currents must be scaled by the product of these two factors, or 25/3, which is found from Ampère's law.

One of the most appealing aspects of the ATF configuration is its MHD stability properties, as shown in Fig. 2 [2]. ATF has enough flexibility in its helical field (HF) and VF coil systems to examine whether the window to the second stability regime exists. An average beta of 9% has been chosen for the reference operating point of ATFSR.

The one major problem area in the scaled-up design is the tight area between the plasma and the HF coils, $\Delta S \simeq 0.4$ m, as shown schematically in Fig. 3 (dimensions and other parameters are given in Table III). A 0.1-m dewar and a 0.05-m first wall thickness are assumed. If ΔS can be increased to 0.6–0.7 m, an efficient shielding material, such as tungsten with boron carbide, can be used directly under the coils [7].

In tokamak plasmas, where very low order harmonics of the poloidal magnetic field are used for shaping, it is relatively easy to

*Research sponsored by the Office of Fusion Energy, U.S. Department of Energy, under Contract No. DE-AC05-84OR21400 with Martin Marietta Energy Systems, Inc.

Table I. Stellarator/Torsatron Power Reactor Designs

	MIT T-2	Japan Heliotron-H	U.S.S.R. TNPP	UW UWTOR-M	LANL MSR-IIB	ORNL ATFSR
Plasma radius (m)	1.5	1.7	2.1	1.72	0.81	1.0
Major radius (m)	24.0	21.0	6.8	24.1	23.0	7.0
Aspect ratio	16.0	12.4	17.5	14.0	28.4	7.0
Plasma volume (m^3)	1067	1198	3203	1407	298	138
Average density ($10^{20}/m^3$)	2.5	1.17	2.5	1.46	3.64	1.2
Average beta	0.065	0.06	0.1	0.06	0.08	0.09
On-axis magnetic field (T)	5.0	4.0	4.4	4.5	6.56	5.0
Peak field at coil (T)	9.0	9.0		11.6	11.6	10.0
First-wall loading (MW/m^2)	2.2	1.3	4.0	1.41	2.0	2.3
Thermal power [MW(t)]	3600	3400	9300	4820	4000	930
Net plant efficiency	0.33	0.31	0.36	0.38	0.33	0.33
Net electric power [MW(e)]	1188	1054	3348	1832	1320	300

DISCLAIMER

ORNL-DWG 85-3124 FED

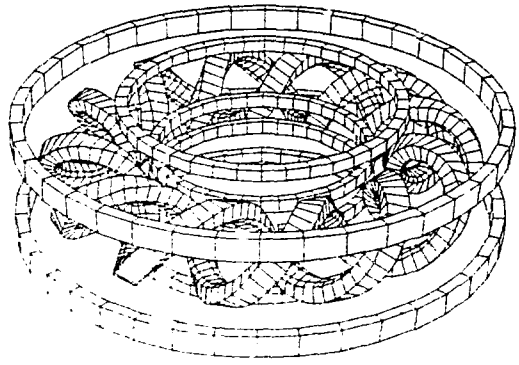

Fig. 1. The ATF-style coil set. The inner, middle, and outer vertical field coils are shown. The middle VF coil system (upper coils inside torus) adds flexibility to the ATF configuration but can be eliminated in ATFSR.

ORNL-DWG 84-2570A FED

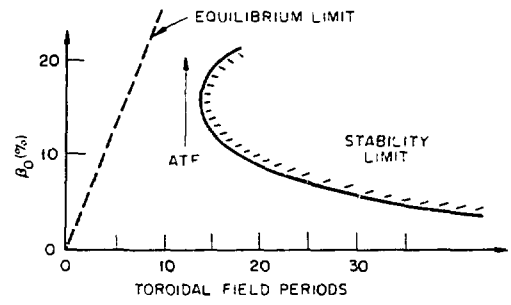

Fig. 2. Combined equilibrium and stability constraints for ATF, showing central β_0 as a function of toroidal field period number. These constraints indicate possible access to the second stability regime at $m = 12$.

Table II. ATF and ATFSR machine parameters

Dimensionless parameters		
Coil configuration	Continuous	
Multipolarity, ℓ	2	
Toroidal field periods, m	12	
Plasma elongation, b_p/a_p	1.65	
Plasma aspect ratio, $R_0/\bar{a}$	7	
Coil aspect ratio, $R_0/\bar{a}_c$	4	
Helical ripple on axis, ϵ_{h0}	0.0	
Helical ripple at edge, ϵ_{ha}	0.22	
Transform on axis, ι_0	0.35	
Transform at edge, ι_a	0.90	
Scaled parameters		
	ATF	ATFSR
Major radius, R_0 (m)	2.1	7.0
Average minor radius, $\bar{a}$ (m)	0.3	1.0
Plasma minor radius, a_p (m)	0.23	0.78
Average coil radius, a_c (m)	0.48	1.75
Major radius of inner VF coils (m)	1.33	4.43
Major radius of outer VF coils (m)	2.94	9.80
Major radius of middle VF coils (m)[a]	1.69	
Vertical position of inner VF coils (m)	±0.20	±0.67
Vertical position of outer VF coils (m)	±0.64	±2.13
Toroidal field on axis, B_0 (T)	2.0	5.0
Helical coil current (MA)	1.75	14.6

[a]Middle VF coils are used to add flexibility to the ATF magnetic configuration. The standard configuration requires no current in these coils.

ORNL-DWG 85-2228 FED

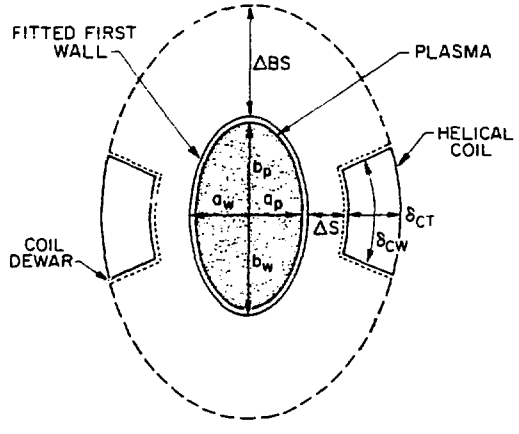

Fig. 3. Schematic cross-sectional view of ATFSR, showing the elliptic plasma (semiminor radius a_p, semimajor radius b_p) with a fitted first wall (semiminor radius a_w, semimajor radius b_w), a coil shield (thickness ΔS), and a blanket (blanket/shield thickness ΔBS). The coil dewars and the helical field coils (thickness δ_{CT}, width δ_{CW}) are shown with the cross sections normal to the coils; the projections of their cross sections in this plane are larger than shown because of the helical pitch of the coils. The plasma chamber rotates poloidally with the toroidal field period number $m = 12$.

move the coils (in minor radius) away from the plasma and allow for a thicker blanket/shield. In stellarators or torsatrons, even small modifications to the HF coils can have a significant effect on the vacuum magnetic field topology. Nonetheless, several options exist to relax the tight spacing of the ATF scaleup: thinner, higher current density coils with the same height and aspect ratio (i.e., the same distance from the coil center to the plasma); lower-aspect-ratio HF coils; a larger-scale device; or some combination of these. Changing either the aspect ratio or the dimensions of the HF coils requires reassessment of the magnetics and a more thorough study than that undertaken here. Lower-aspect-ratio coil designs that preserve the desirable MHD characteristics of ATF are under investigation [8].

The HF coils in ATF are designed for 28 MA/m^2 in the copper or about 20 MA/m^2 averaged over the coil, including structure and cooling channels. The scaleup to ATFSR leads to a reduction in HF coil current density to ~15 MA/m^2. The field at the coil is twice that on axis, $B_c \simeq 10$ T, so the design is comfortably within the limits for pool boiling in NbTi superconductor magnets (≃18–20 MA/m^2). Forced flow in Nb_3Sn could raise the limit to ≃40 MA/m^2 [9].

Table III. ATFSR blanket, shield, and coil parameters

First-wall configuration	Fitted
Wall semiminor radius, a_w (m)	0.86
Wall semimajor radius, b_w (m)	1.37
Wall surface area, S_w (m^2)	276
First-wall thickness (m)	0.05
Dewar thickness (m)	0.1
Coil shield thickness, ΔS (m)	0.4
Blanket-shield thickness, ΔBS (m)	1.5
Field at coil, B_{max} (T)	10
Maximum current density (MA/m^2)	15
Coil thickness, δ_{CT} (m)	0.7
Coil width, δ_{CW} (m)	1.4

The chamber wall is shown as fitted to the plasma in Fig. 3. Since space is not a restriction at the top and bottom as shown in the figure (rotated poloidally with movement toroidally around the machine), room can be made for an expanded boundary or divertor [10] to collect particles and energy; for diagnostic, fueling, and heating ports; etc.

III. Confinement

The confinement properties of ATFSR were examined with the POPCON option in the WHIST transport code [11]. The particle and energy transport equations are essentially those used in tokamak analysis but with the radial electric field effects incorporated into the radial fluxes.

In axisymmetric plasmas, the radial electric field term is ignored since the neoclassical fluxes of ions and electrons are intrinsically ambipolar. In a nonaxisymmetric plasma, however, the fluxes of ions and electrons are not generally equal, so a slight charge separation builds up and an electric potential forms. The resulting radial electric field ($-\phi'$) introduces a poloidal ($\mathbf{E} \times \mathbf{B}$) drift that detraps particles and therefore reduces the loss of ripple-trapped particles [12].

We present two means of incorporating the radial electric field in our analysis: (1) assuming a parabolic profile for the electric potential normalized to the central ion temperature,

$$\xi = kT_i\big|_{\rho=0}(\rho/\bar{a})^2 ,$$

and (2) solving for a self-consistent radial electric potential from the neoclassical particle fluxes [5].

A Gaussian heating profile with a half-width of $\bar{a}/2$ and with 25% of the power delivered to the electrons and 75% to the thermal ions was used to simulate ion cyclotron resonant heating (ICRH) in the evaluation of auxiliary power needs for startup. Pellet fueling maintained equal densities of deuterium and tritium through feedback on the source.

Figure 4 shows the operating contours, plotted in $\langle n_e \rangle$–$\langle T \rangle$ space, for a large potential ($\xi = 4$), where

$$\langle T \rangle = \frac{1}{\langle n_e \rangle}\frac{1}{2V}\int dV\,(n_eT_e + n_iT_i)$$

and $\langle n_e \rangle$ is the volume-averaged electron density. Ignition ($P^{eq}_{aux} = 0$) occurs at $\langle \beta_T \rangle \simeq 8\%$ with a fusion power output of about

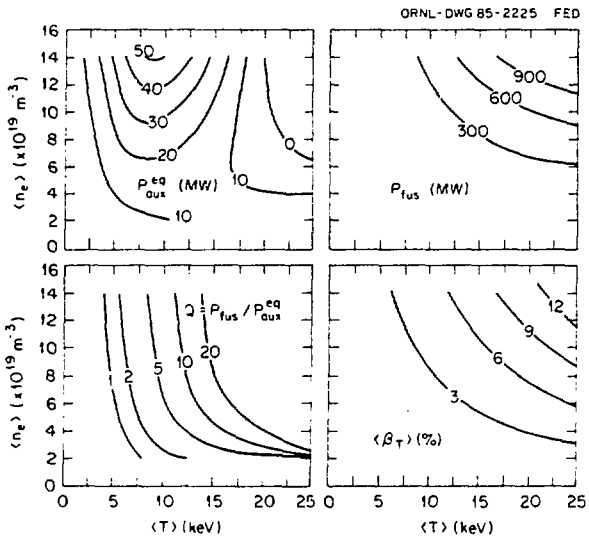

Fig. 4. Steady-state contours for an assumed electric potential profile characterized by $\xi = 4$. The contours are supplementary heating (P^{eq}_{aux}), fusion power (P_{fus}), Q (P_{fus}/P^{eq}_{aux}), and toroidal beta ($\langle \beta_T \rangle$).

300 MW. The reference operating values of Table I are obtained at the intersection of the ignition curve and the $\langle \beta_T \rangle = 9\%$ contour. A recirculating power fraction of 5%, a thermal conversion efficiency of 33%, and an energy multiplication factor of 1.2 in the blanket are also assumed. The electron energy confinement time is ~0.5 s, and the ion energy confinement time is ~5 s for a net global energy confinement time of 0.9 s—comparable to that for a tokamak of the same size.

Since stellarators can run steady-state, startup is infrequent, and there is no strong limitation on the startup time; the minimum in the steady-state auxiliary power contours between the origin (i.e., at $\langle \beta_T \rangle \simeq 0$) and the ignition curve then closely approximates the startup power requirements [11]. In this case, about 20 MW is required for a low-density, ramped startup.

The same analysis with lower electric potential ($\xi = 2$) raises the ignition curve above $\langle \beta_T \rangle = 9\%$. At the reference operating point, $Q \simeq 15$ and the global confinement is ≃0.7 s; thus, about 50 MW of steady-state auxiliary power is required. At $\xi \simeq 3$ the ignition curve just intersects the 9% beta curve, giving a single-point operating window (ignition margin of 1).

At low temperatures (high collisionality), the neoclassical ion particle losses dominate and yield a negative ambipolar electric potential. On the other hand, in the higher-temperature, lower-collisionality regime of a reactor, the electron losses dominate, and a positive potential is obtained. This leads to a necessary transition through small potentials and electric fields where resonant neoclassical helical ripple losses are expected to be large. For the case presented in Fig. 5 the potential in this transition zone is calculated and allowed to asymptotically approach $\xi = 4$ at high temperatures where the neoclassical ripple-induced fluxes are reduced. The $\phi = 0$ transition occurs along a curve roughly intersecting the bottoms of the auxiliary power contours and strengthens the requirement of a low-density startup. At a density of $\langle n_e \rangle \simeq 2 \times 10^{19}$ m^{-3}, an auxiliary power of ≃20 MW (contour not shown) can be used to force the transition to the low-collisionality, electron-dominated loss solution at a low temperature (≃5 keV) where the conduction losses are not very severe. As the density is increased the transition occurs at higher temperatures, with the resonant losses increasing rapidly.

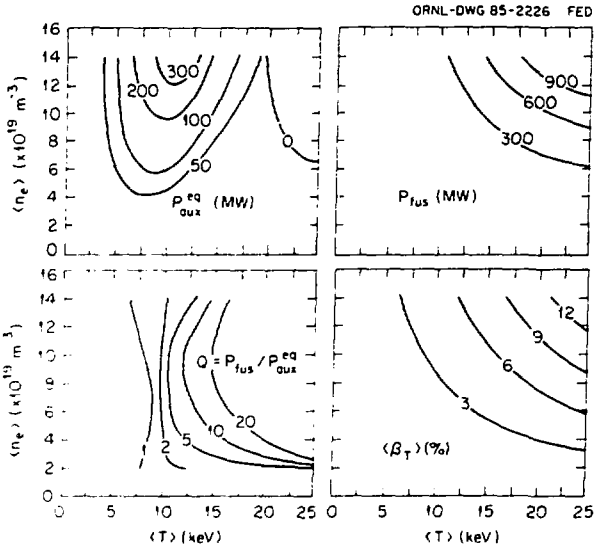

Fig. 5. Steady-state contours with self-consistent E_r evolution through the transition and $\xi = 4$ thereafter. The contours are those described in Fig. 4.

IV. Summary

Emphasis has been placed in this study on a low-aspect-ratio torsatron configuration that has high-beta capabilities and thus leads to an attractive reactor regime. Blanket/shield space under the helical coils is not adequate, but helical coils with a slightly lower aspect ratio (reduced from $\simeq$4 to $\simeq$3.7–3.8), coupled with increased coil current density, could solve this problem.

Although recent theoretical MHD stability and confinement results have been used, it must be emphasized that the physics has been extended into an experimentally untried regime where new phenomena are predicted (high beta through direct access to the second stability regime and an electron-dominated collisionless neoclassical transport regime). For example, neoclassical ripple-induced losses of thermal particles have been used to evaluate a "self-consistent" radial electric field. However, nonambipolar "anomalous" losses or a nonthermal, anisotropic tail on either the electron or ion distribution function driven by auxiliary heating may dominate the particle losses and govern the potential (e.g., as shown by the Wendelstein VII-A beam injection experiments [6]). The choice of auxiliary heating (neutral beams, ECRH, ICRH, etc.) may well provide some external control of the ambipolar potential and therefore of the confinement of thermal particles.

References

[1] J. F. Lyon, B. A. Carreras, K. K. Chipley, M. J. Cole, J. H. Harris, T. C. Jernigan, R. L. Johnson, V. E. Lynch, B. E. Nelson, J. A. Rome, J. Sheffield, and P. B. Thompson, "Physics Optimization, Engineering Design and Operational Capabilities of the ATF Torsatron," *Fusion Technol.*, accepted for publication (1986).

[2] B. A. Carreras, H. R. Hicks, J. A. Holmes, V. E. Lynch, L. Garcia, J. H. Harris, T. C. Hender, and B. F. Masden, "Equilibrium and Stability Properties of High-Beta Torsatrons," *Phys. Fluids* **26** (1983) 3569–79.

[3] R. L. Miller, "Recent Progress in Stellarator Reactor Conceptual Design," *Fusion Technol.* **8** (1985) 1581–9.

[4] J. T. Lacatski, W. A. Houlberg, and N. A. Uckan, "Plasma Engineering Analysis of a Small Torsatron Reactor," ORNL/TM-9533, Oak Ridge National Laboratory (1985).

[5] D. E. Hastings, W. A. Houlberg, and K. C. Shaing, "The Ambipolar Electric Field in Stellarators," *Nucl. Fusion* **25** (1985) 445–54.

[6] W VII-A Team: G. Cattanei, D. Dorst, A. Elsner, V. Erckmann, G. Grieger, P. Grigull, H. Hacker, H. J. Hartfuss, M. A. Hellberg, H. Jäckel, R. Jaenicke, J. Junker, M. Kick, H. Kroiss, G. Kuehner, H. Maassberg, C. Mahn, S. Marlier, G. Müller, W. Ohlendorf, F. Rau, H. Renner, H. Ringler, F. Sardei, M. Tutter, A. Weller, H. Wobig, E. Würsching, M. Zippe, K. Freudenberger, W. Ott, F.-P. Penningsfeld, E. Speth, and H. Büchl, in "Plasma Confinement and the Effect of Rotational Transform in the Wendelstein VII-A Stellarator," in *Plasma Physics and Controlled Nuclear Fusion Research (Proc. 10th Int. Conf. London, 1984)*, Vol. 2, IAEA, Vienna (1985) 371–82.

[7] C. C. Baker et al., "STARFIRE: A Commercial Fusion Tokamak Power Plant Study," ANL/FPP-80-1, Argonne National Laboratory (1980).

[8] J. H. Harris, Oak Ridge National Laboratory, private communication (1985).

[9] J. Sheffield, R. A. Dory, S. M. Cohn, J. G. Delene, L. Parsly, D. E. T. F. Ashby, and W. T. Reiersen, "Cost Assessment of a Generic Magnetic Fusion Reactor," ORNL/TM-9311, Oak Ridge National Laboratory (1985); to be published in *Fusion Technol.*

[10] R. Sanders and I. N. Sviatoslavski, "Divertor Target Design for the UWTOR-M Modular Stellarator Power Reactor," *Nucl. Technol./Fusion* **4**, Pt. 3 (1983) 993–7.

[11] W. A. Houlberg, S. E. Attenberger, and L. M. Hively, "Contour Analysis of Fusion Reactor Plasma Performance," *Nucl. Fusion* **22** (1982) 935–45.

[12] K. C. Shaing, R. H. Fowler, D. E. Hastings, W. A. Houlberg, E. F. Jaeger, J. F. Lyon, J. A. Rome, J. S. Tolliver, "The Radial Electric Field in a Non-Axisymmetric Torus," in *Plasma Physics and Controlled Nuclear Fusion Research (Proc. 10th Int. Conf. London, 1984)*, Vol. 2, IAEA, Vienna (1985) 189–95.